A Position Stepping Method for Predicting Performances of Switched Reluctance Motor Drives

X. D. Xue, K. W. E. Cheng, *Senior Member, IEEE*, and S. L. Ho

***Abstract*—This paper presents a novel numerical method, which will be referred as the position stepping method (PSM), to predict the performances of switched reluctance motor (SRM) drives. The 2-D bicubic spline is employed to generate the finite rectangular elements. The 2-D bilinear spline is used to model the nonlinear magnetic characteristics in SRMs. Consequently, the conventional nonlinear first-order differential voltage equation for describing the performances of SRM drives can be simplified into an analytical expression in terms of the current with respect to the rotor position. Furthermore, the position stepping algorithm is developed according to the boundary and continuity conditions, to accurately and rapidly compute the current from the proposed current expression. Simulated and measured current waveforms are reported to validate the developed PSM. The CPU execution time required by the PSM compares very favorably with that of the analytical method. Overall, this paper provides an accurate and speedy approach to predict the currents and torques of SRM drives.**

***Index Terms*—Modeling, nonlinear magnetics, simulation, spline, switched reluctance motors (SRMs).**

NOMENCLATURE

$\boldsymbol{A}$	4×4 coefficients matrix in bicubic spline function.
a_{xyjl} $(j,l=1,2,3,4)$	Coefficients of matrix in bicubic spline function.
c_{kj}	Coefficients in element shape function.
D_{kj}	Integration constant on element.
E_{xy}	Subrectangular element on plane domain being composed of rotor position and current.
g_{xl} and g_{yl} $(l=1,2,3,4)$	Polynomials in bicubic spline function.
i	Phase winding current.
$i_{\max}$	Maximum phase current.
M	Number of given phase currents.
MM	Number of currents generated by bicubic spline interpolation.
N	Number of given rotor positions.
NN	Number of rotor positions generated by bicubic spline interpolation.
R	Resistance of phase winding.
t	Time.
T	Instantaneous torque produced by an SRM.
T_{ph}	Instantaneous torque produced by a phase.
W'	Coenergy.
V	Voltage applied to phase winding.
θ	Rotor angular position.
θ_b	Rotor position on the boundary between two adjacent elements.
θ_{on}	Turn-on angle.
θ_p	Period of rotor position.
Ω	Plane domain being composed of rotor position and current.
Ω_{kj}	Element generated by bicubic spline interpolation.
$\bar{\Omega}_{kj}$	Element next to Ω_{kj}.
ω_r	Motor speed.
ψ	Flux linkage.
$\psi_{kj}(\theta,i)$ $(k,j=1,2)$	Element shape function.

Manuscript received January 10, 2006; revised August 21, 2006. This work was supported by the Research Committee of the Hong Kong Polytechnic University under Project G-YX52. Paper no. TEC-00453-2005.

The authors are with the Department of Electrical Engineering, Hong Kong Polytechnic University, Kowloon, Hong Kong (e-mail: eexdxue@polyu.edu.hk; eeecheng@polyu.edu.hk; eeslho@polyu.edu.hk).

Digital Object Identifier 10.1109/TEC.2007.895859

I. INTRODUCTION

COMPUTED-AIDED design, performance prediction, and torque control of switched reluctance motors (SRMs) require accurate modeling of SRMs and rapid simulation. Accurate modeling of SRMs depend on how accurately the magnetic characteristics in SRMs are described. An SRM usually operates in the magnetic flux saturation region so as to realize a high torque-to-mass ratio. Thus, magnetic saturation is essential in high-performance SRMs. However, high-magnetic saturation and doubly salient poles in SRMs imply that the flux linkage or inductance characteristics in SRMs are nonlinear functions of both the rotor position and the phase current. Naturally, the nonlinear flux linkage or inductance in SRMs make the modeling of SRMs nonlinear, which is used to describe the SRM operation. The model to predict the performances of SRM drives is given by

$$\frac{d\psi}{dt} = V - Ri \tag{1}$$

where ψ is the flux linkage, t is the time, V is the voltage applied to a phase winding, R is the resistance of a phase winding, and i is the phase current.

Clearly, the accuracy and rapidity of predicting the performance or simulation of SRM drives depend on both the modeling of the magnetic characteristics and the solution to the nonlinear first-order differential voltage equation (1).

A number of studies have focused on the modeling of magnetic characteristics in SRMs. Depending on the methodologies

to establish modeling of nonlinear magnetic characteristics in SRMs, they may be classified into four kinds [1].

A. Analytical Models

In such models, proper analytical expressions are used to characterize the nonlinearities of phase flux linkage or inductance versus both phase current and rotor position. Using such models, the nonlinear magnetic characteristics are computed easily and rapidly. Torrey and Lang presented an analytical expression of the flux linkage with respect to the rotor position and current. In the expression, the flux linkage is a compound function of the Fourier series and an exponent with respect to the rotor position and current [2]. Chan and Weldon [3] proposed a complicated 2-D function using series and exponential components to curve-fit the flux linkage data of SRMs. Fahimi *et al*. presented a new analytical model in which the dependency of the phase inductance on position is represented by a limited number of Fourier series terms, and the nonlinear variation of the inductance with the phase current is expressed by means of polynomial functions [4]. Mir *et al*. used a compound analytical model consisting of both exponential and sinusoidal functions, and the model can implement on-line parameter identification [5]. Roux and Morcos [6] presented an SRM model which produces a piecewise analytical expression of phase flux linkage with respect to both the phase current and the rotor position. An improved analytical model was presented by Essah and Sudhoff in which the reciprocal of the inductance is expressed as a polynomial with respect to the flux linkage, and the coefficients in the polynomial are computed form the Fourier series with respect to the rotor position [7]. Xue *et al*. developed an analytical model of magnetic characteristics, which is composed of the 2-D least square polynomials with respect to the rotor position and current [8]. Loop *et al*. proposed the alternative model of SRMs, named as the nonlinear average value model (NLAM). By introducing the state variables that are constant in the steady state, the analytical expressions of the current and torque are derived [9].

B. Interpolation Models

In such models, the given nonlinear magnetic data of SRMs are stored in tabular forms, and the phase flux linkage or inductance is interpolated with appropriate piecewise interpolation methods. The salient advantage of the interpolation models is that they are able to accurately describe the nonlinear magnetic characteristics of SRMs by virtue of the good interpolation methods, such as the model proposed by Stephenson and Corda [10]. In their model, the magnetic data are stored in tabular form, the flux linkage with respect to the current is interpolated with a quadratic interpolation method, and the rotor position is interpolated linearly for a specified phase current. Pulle further improved the method using cubic spline to interpolate the flux linkage with respect to the phase current for a set of discrete rotor position values. The quadratic interpolation is employed to compute the flux linkage with respect to the rotor position for a set of discrete current values [11]. Rehman and Taylor presented a piecewise interpolation model to characterize the nonlinearities of magnetic data based on the bilinear interpolation method [12]. Xue *et al*. also proposed the use of a 2-D bicubic spline to interpolate the flux linkage with respect to the rotor position and current to simulate an SRM drive [13].

C. Models Based on Artificial Neural Network (ANN) Methods

Such models are trained by a large number of given discrete magnetic data before being employed to describe the nonlinear magnetic characteristics of SRMs. The accuracy of ANN models is mainly dependent on the amount of the given magnetic data. Elimas *et al*. proposed the use of ANNs to model the magnetic nonlinearities of SRMs using back-propagation algorithm [14]. Belfore and Arkadan used evolutionary neural networks (ENNs) to develop an SRM model [15]. Arkadan *et al*. proposed the use of a genetic-algorithm-based ANN to predict the characteristics of SRMs [16].

D. Models Based on Equivalent Magnetic Circuit Methods

These models are used to describe the nonlinear magnetic characteristics of SRMs by using analytical expressions based on equivalent magnetic circuits together with permeance. The computation of magnetic characteristics is fast when using these models. However, the accuracy is limited by equivalent magnetic circuit. Radun used a magnetic circuit concept to present an analytical expression of the flux linkage to predict the performance, and to guide the design of an SRM [17]. Moallem and Dawson used a magnetic equivalent circuit method to model the nonlinear characteristics of SRMs [18]. Vujicic and Vukosavic presented a nonlinear SRM model based on equivalent magnetic circuit using a set of reluctances that are linked in series and in parallel [19].

Reported solutions to the first-order differential voltage equation (1) may be summarized in three approaches: 1) the Euler integration method; 2) the fourth-order Runge–Kutta method; and 3) using commercial softwares that generally use approximate numerical algorithms, such as Simulink. When using these solution methods, there are two unavoidable drawbacks. One is that these methods are based on the use of approximate numerical algorithms in solving first-order differential equation, and hence, they will result in inherent errors arising from mathematical approximation. The other drawback is that at each iteration step it is necessary to compute the current from the solved flux linkage or the inductance from the solved current, and thus, the computation burden is very heavy.

In this paper, a new method that is referred as the position stepping method (PSM), is proposed to predict the performances of SRM drives. The PSM is based on a proposed hybrid model to describe the nonlinear magnetic characteristics. The hybrid model is different from the previously reported modeling and the main improvements are as follows:

1) It only requires a small quantity of given magnetic data obtained from the experiments or from the numerical computation such as finite element (FE) analysis. The finite fine rectangular elements are generated automatically using a

2-D bicubic spline interpolation from the given magnetic data.

2) The 2-D bilinear spline function is defined as the element shape function on each such element, so to model the relationship between the flux linkage in terms of both the rotor position and the current.
3) The aforementioned shape function is applied to the first-order differential voltage equation for SRM drives. Consequently, the conventional first-order differential voltage equation can be simplified into an analytical expression of the current with respect to the rotor position.
4) From the boundary value condition and the continuity condition of the current, a position stepping algorithm is developed to accurately and speedily solve the above analytical expression.

Thus, the developed PSM is able to simplify the conventional first-order differential voltage equation for SRM drives into an analytical expression of the current in terms of the rotor position. Furthermore, the PSM can be used to compute the SRM current and torque from the developed expressions rapidly and accurately. On the other hand, the hybrid model using both the 2-D bicubic spline interpolation and the 2-D bilinear shape function can be utilized to accurately characterize the nonlinear magnetic behaviors in SRMs. Therefore, the main advantage of the proposed algorithm is its accuracy and rapidity in obtaining the simulation solutions. Both experimental and simulation results are reported to validate the proposed hybrid model and the PSM.

II. Hybrid Model of Nonlinear Magnetic Characteristics

A. Automatic Generation of Rectangular Elements Based on 2-D Bicubic Spline Interpolation

The flux linkage is a function of both the rotor position angle θ and the phase current i for SRMs. In general, θ and i vary separately within the limited regions. In this paper, it is assumed that the computation region of θ is limited within one period θ_p, i.e., $\theta_{\rm on} \le \theta \le (\theta_{\rm on} + \theta_p)$, and the computation region of i is limited from 0 to the maximum value $i_{\max}$, i.e., $0 \le i \le i_{\max}$, where $\theta_{\rm on}$ represents the turn-on angle. The rotor position angle θ is equal to zero when the stator pole is unaligned with the rotor pole. It is clear that the plane domain Ω being composed of θ and i is a rectangular domain.

Suppose that a limited number of discrete data of magnetic characteristics are obtained experimentally or from FE analysis. One has $\theta_{\rm on} = \theta_1 < \theta_2 < \cdots < \theta_N = (\theta_{\rm on} + \theta_p)\,(N \ge 2)$ and $0 = i_1 < i_2 < \cdots < i_M = i_{\max}(M \ge 2)$, where N represents the number of the given rotor position angles and M represents the number of the given phase currents. Hence, there are $N \times M$ grid points in the rectangular domain Ω. Moreover, Ω is subdivided into $(N-1) \times (M-1)$ sub-rectangles $E_{xy}(x = 1, 2, \ldots, N-1$ and $y = 1, 2, \ldots, M-1)$ with vertices at $(\theta_x, i_y), (\theta_{x+1}, i_y), (\theta_{x+1}, i_{y+1})$ and (θ_x, i_{y+1}), which are referred as the elements. Fig. 1 illustrates the configuration of the element $E_{\rm xy}$ for the 2-D bicubic spline interpolation.

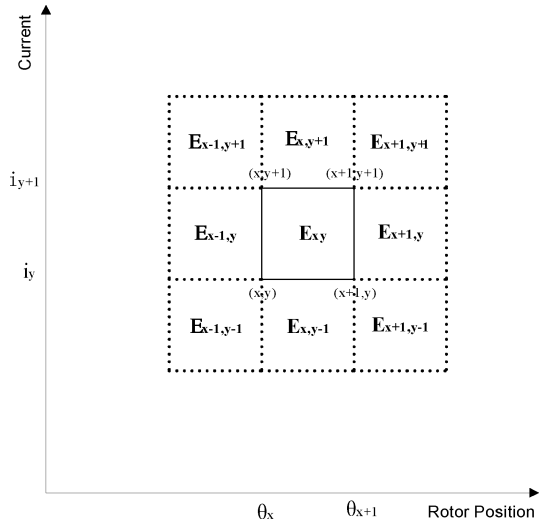

Fig. 1. Configuration of the element E_{xy} for the 2-D bicubic spline interpolation.

For the each aforementioned element $E_{\rm xy}$, the 2-D bicubic spline interpolation function can be given by [20]

$$\psi_{\rm xy}(\theta, i) = (g_{x1}(\theta), g_{x2}(\theta), g_{x3}(\theta), g_{x4}(\theta))\boldsymbol{A}\begin{pmatrix} g_{y1}(i) \\ g_{y2}(i) \\ g_{y3}(i) \\ g_{y4}(i) \end{pmatrix} \tag{2}$$

where the g_{xl} and g_{yl} are $(l = 1, 2, 3, 4)$ defined by

$$\begin{aligned} &g_{x1} = 1, \quad g_{y1} = 1 \\ &g_{x2} = \theta - \theta_x, \quad g_{y2} = i - i_y \\ &g_{x3} = (\theta - \theta_x)^2, \quad g_{y3} = (i - i_y)^2 \\ &g_{x4} = (\theta - \theta_x)^3, \quad g_{y4} = (i - i_y)^3 \end{aligned} \tag{3}$$

and $\boldsymbol{A}$ is the 4×4 coefficients matrix, which is expressed by

$$\boldsymbol{A} = \begin{pmatrix} a_{xy11} & a_{xy12} & a_{xy13} & a_{xy14} \\ a_{xy21} & a_{xy22} & a_{xy23} & a_{xy24} \\ a_{xy31} & a_{xy32} & a_{xy33} & a_{xy34} \\ a_{xy41} & a_{xy42} & a_{xy43} & a_{xy44} \end{pmatrix}. \tag{4}$$

The coefficients in $\boldsymbol{A}$ are computed using the given flux linkage values and the values of the both first-partial and mixed-partial derivative at each of the four nodes of E_{xy} [13], [20]. Using (2), the flux linkage at any position and any current in Ω can be computed. Thus, 'finer' finite elements can be generated automatically. The results of the element generation may be described as follows: $(\text{NN}-1) \times (\text{MM}-1)$ rectangular elements in Ω are generated. For the rotor position there is $\theta_{\rm on} = \theta_1 < \theta_2 < \cdots < \theta_{\rm NN} = (\theta_{\rm on} + \theta_p)\,(\text{NN} \ge N)$. For the current there is $0 = i_1 < i_2 < \cdots < i_{\rm MM} = i_{\max}(\text{MM} \ge M)$. NN represents the number of the generated rotor positions, and MM represents the number of the generated phase currents. Hence, the arbitrary element Ω_{kj} has vertices at $(\theta_k, i_j), (\theta_{k+1}, i_j), (\theta_{k+1}, i_{j+1})$ and (θ_k, i_{j+1}), where $1 \le k \le (\text{NN}-1)$ and $1 \le j \le (\text{MM}-1)$. The corresponding flux

linkage values are $\psi(\theta_k, i_j), \psi(\theta_{k+1}, i_j), \psi(\theta_{k+1}, i_{j+1})$ and $\psi(\theta_k, i_{j+1})$.

B. Element Shape Function Based on 2-D Bilinear Spline Function

Using the 2-D bilinear spline function, the shape function defined on the element Ω_{kj} is determined by [20]

$$\psi_{kj}(\theta, i) = c_{kj11} + c_{kj21}\theta + c_{kj12}i + c_{kj22}i\theta \tag{5}$$

where

$$\begin{aligned} c_{kj11} &= b_1 - b_2\theta_k/\Delta\theta_k - b_3 i_j/\Delta i_j + b_4\theta_k i_j/(\Delta\theta_k \Delta i_j) \\ c_{kj21} &= b_2/\Delta\theta_k - b_4 i_j/(\Delta\theta_k \Delta i_j) \\ c_{kj12} &= b_3/\Delta i_j - b_4\theta_k/(\Delta\theta_k \Delta i_j) \\ c_{kj22} &= b_4/(\Delta\theta_k \Delta i_j) \end{aligned} \tag{6}$$

and

$$\begin{aligned} b_1 &= \psi(\theta_k, i_j) \\ b_2 &= \psi(\theta_{k+1}, i_j) - \psi(\theta_k, i_j) \\ b_3 &= \psi(\theta_k, i_{j+1}) - \psi(\theta_k, i_j) \\ b_4 &= \psi(\theta_{k+1}, i_{j+1}) - \psi(\theta_k, i_{j+1}) - \psi(\theta_{k+1}, i_j) + \psi(\theta_k, i_j) \\ \Delta\theta_k &= \theta_{k+1} - \theta_k \\ \Delta i_j &= i_{j+1} - i_j. \end{aligned} \tag{7}$$

It can be seen from (5) to (7) that the proposed analytical model to describe the nonlinear magnetic characteristics is based on the elements generated using the 2-D bicubic spline interpolation. Thus, the proposed model is a hybrid model.

III. PSM

A. First-Order Differential Voltage Equation at Steady State

Assuming that an SRM is supplied by a voltage source and the mutual coupling is negligible, its first-order differential voltage equation at steady state can be expressed by

$$\frac{d\psi(\theta, i)}{d\theta} = \frac{1}{\omega_r}(V - Ri) \tag{8}$$

where ω_r denotes the motor speed.

B. Simplifying the First-Order Differential Voltage Equation

By substituting (5) into (8), we get

$$(c_{kj12} + c_{kj22}\theta)\frac{di}{d\theta} + (c_{kj22} + R/\omega_r)i = V/\omega_r - c_{kj21} \tag{9}$$

where $\theta_k \le \theta \le \theta_{k+1}, i_j \le i \le i_{j+1}, k = 1, 2, \ldots, (\text{NN} - 1)$, and $j = 1, 2, \ldots, (\text{MM} - 1)$.
If

$$P(\theta) = (c_{kj22} + R/\omega_r)/(c_{kj12} + c_{kj22}\theta) \tag{10}$$

and

$$Q(\theta) = (V/\omega_r - c_{kj21})/(c_{kj12} + c_{kj22}\theta). \tag{11}$$

Then, (9) can be changed into

$$\frac{di}{d\theta} + P(\theta)i = Q(\theta). \tag{12}$$

Equation (12) is the typical first-order differential equation. Its analytical solution can be expressed by

$$i(\theta)_{\in\Omega_{kj}} = e^{-\int P(\theta)d\theta}\left(\int Q(\theta)e^{\int P(\theta)d\theta}d\theta + D_{kj}\right) \tag{13}$$

where D_{kj} is the integration constant defined on the element $\Omega_{kj}, \theta_k \le \theta \le \theta_{k+1}, i_j \le i \le i_{j+1}, k = 1, 2, \ldots, (\text{NN} - 1)$, and $j = 1, 2, \ldots, (\text{MM} - 1)$.

From (10), we have

$$\int P(\theta)d\theta = \frac{c_{kj22} + R/\omega_r}{c_{kj22}} \ln|c_{kj12} + c_{kj22}\theta|. \tag{14}$$

Similarly, from (11) we can have

$$\begin{aligned} \int Q(\theta)e^{\int P(\theta)d\theta}d\theta = &\frac{V/\omega_r - c_{kj21}}{c_{kj22}(1 + R/(\omega_r c_{kj22}))} \\ &\times |c_{kj12} + c_{kj22}\theta|^{(1+R/(\omega_r c_{kj22}))} \end{aligned} \tag{15}$$

Substituting both (14) and (15) into (13) gives

$$\begin{aligned} i(\theta)_{\in\Omega_{kj}} = &\frac{V/\omega_r - c_{kj21}}{c_{kj22}(1 + R/(\omega_r c_{kj22}))} \\ &+ D_{kj}\,|c_{kj12} + c_{kj22}\theta|^{-(1+R/(\omega_r c_{kj22}))}. \end{aligned} \tag{16}$$

The model of SRMs proposed in this paper is represented by (16). It can be found from (8) and (16) that the conventional first-order differential voltage equation for SRMs can be simplified into an analytical expression of the current with respect to the rotor position. The current can be computed from (16) if the integration constant D_{kj} on the element Ω_{kj} is determined.

C. Boundary Condition, Continuity Condition, and Element Integration Constant

For an SRM, the boundary condition of the current is the initial value condition of the current. In this study, the starting point of the rotor position is selected as the turn-on angle. Hence, such an initial value condition is determined by

$$i(\theta_1) = i(\theta_{\text{on}}) = 0. \tag{17}$$

The phase current varies continually in the whole domain Ω. Hence, the phase current also changes continually on the boundaries between two adjacent elements. For the arbitrary element Ω_{kj}, the continuity condition must be one of these five cases illustrated in Fig. 2.

From Fig. 2, the continuity condition of the current can also be expressed by any of the following five conditions:

$$\begin{cases} i(\theta_b)_{\in\Omega_{kj}} = i(\theta_b)_{\in\Omega_{k,j+1}}, & (\theta_k < \theta_b < \theta_{k+1}) \\ i(\theta_{k+1})_{\in\Omega_{kj}} = i(\theta_{k+1})_{\in\Omega_{k+1,j+1}}, & (\theta_b = \theta_{k+1}) \\ i(\theta_{k+1})_{\in\Omega_{kj}} = i(\theta_{k+1})_{\in\Omega_{k+1,j}}, & (\theta_b = \theta_{k+1}) \\ i(\theta_{k+1})_{\in\Omega_{kj}} = i(\theta_{k+1})_{\in\Omega_{k+1,j-1}}, & (\theta_b = \theta_{k+1}) \\ i(\theta_b)_{\in\Omega_{kj}} = i(\theta_b)_{\in\Omega_{k,j-1}}, & (\theta_k < \theta_b < \theta_{k+1}) \end{cases} \tag{18}$$

where θ_b is the rotor position value on the boundary between two adjacent elements.

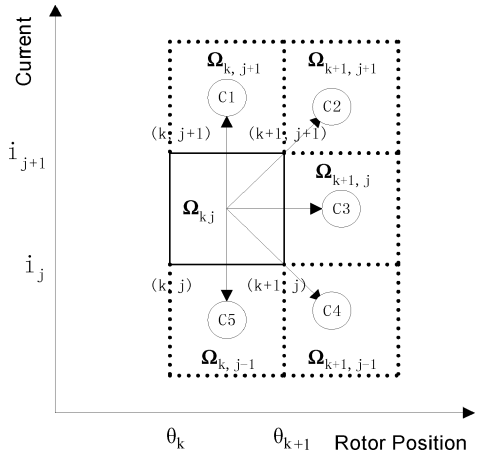

Fig. 2. Schematic diagram of the continuity condition of the current for the arbitrary element Ω_{kj}.

From both (16) and (18), the integration constant D_{kj} defined on the element Ω_{kj} can be computed as

$$D_{kj\in\Omega_{kj}} = (i(\theta_b)_{\in\bar{\Omega}_{kj}} - \frac{V/\omega_r - c_{kj21}}{c_{kj22}(1 + R/(\omega_r c_{kj22}))}) \times |c_{kj12} + c_{kj22}\theta_b|^{(1+R/(\omega_r c_{kj22}))} \quad (19)$$

where $\bar{\Omega}_{kj}$ represents the last element next to Ω_{kj}.

D. Position Stepping Algorithm

To compute the current from (16), (17), and (19), an efficient solution algorithm referred as the position stepping algorithm is developed in this paper. Fig. 3 shows the flowchart diagram of this algorithm. The algorithm is executed as follows:

1) The initial position is selected as the turn-on angle. Consequently, for the first element $\Omega_{11}(k = 1$ and $j = 1)$, there are $\theta_k = \theta_1 = \theta_{\rm on}$ and $i_j = i_1 = i(\theta_1) = i(\theta_{\rm on}) = 0$. It can be seen that the initial current value and the initial position value for the first element are the given values, respectively.
2) The coefficients $c_{kjpq}(p$ or $q = 1, 2)$ in the element Ω_{kj} are computed. In the meantime, the integration constant D_{kj} in the element Ω_{kj} is also computed from (19). For $k = 1$ and $j = 1$, there is $i(\theta_b) = i(\theta_1) = 0$.
3) The position increases by a step size to give the present position.
4) The position stepping algorithm ends if the present position reaches the given final position $\theta_{\rm NN}$. Otherwise, it goes to (5).
5) If the present position is larger than the position θ_{k+1}, it indicates that the present position is not in the element Ω_{kj}, hence, the current at the position θ_{k+1} needs to be computed from (16), and then, it goes to (6). Otherwise, it indicates that the present position is still within the element Ω_{kj}. Hence, the current at the present position is computed from (16) and then, it goes to (8).
6) If the current value is equal to the value i_{j+1}, the second kind of continuity condition can be determined from (18), and θ_b is equal to θ_{k+1}. Hence, the new element $\Omega_{kj}(k = k + 1$ and $j = j + 1)$ can be obtained, and then, it goes to (10). Otherwise, it goes to (7).
7) If the current is larger than the value i_j and smaller than i_{j+1}, the third kind of continuity condition can be determined from (18), and θ_b is equal to θ_{k+1}. Thus, the new element $\Omega_{kj}(k = k + 1$ and $j = j)$ can be obtained, and then, it goes to (10). Otherwise, the fourth kind of continuity condition can be determined from (18), and θ_b is equal to θ_{k+1}. Hence, the new element $\Omega_{kj}(k = k + 1$ and $j = j - 1)$ can be obtained, and then, it goes to (10).
8) If the current value is larger than the value i_{j+1}, the first kind of continuity condition can be determined from (18), and θ_b must be larger than θ_k and smaller than θ_{k+1}. From (16), θ_b can be computed using bisection algorithm when the current is equal to i_{j+1}. Hence, the new element $\Omega_{kj}(k = k$ and $j = j + 1)$ can be obtained, and then, it goes to (10). Otherwise, it goes to (9).
9) If the current value is smaller than the value i_j, the fifth kind of continuity condition can be determined from (18), and θ_b must be larger than θ_k and smaller than θ_{k+1}. From (16), θ_b can be computed using bisection algorithm when the current is equal to i_j. Hence, the new element Ω_{kj} $(k = k$ and $j = j - 1)$ can be obtained, and then, it goes to (10). Otherwise, it indicates that the computed current at the present position is true, and the current at the next position should then be computed. Hence, it goes back to (3).
10) It indicates that the computed current at the present position is false and must be recomputed. Therefore, the

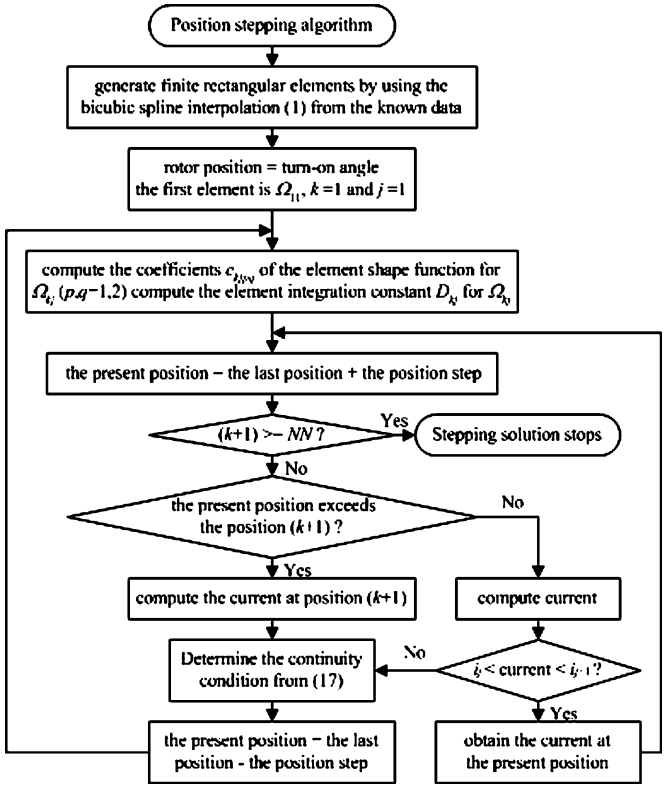

Fig. 3. Flowchart diagram of the proposed position stepping algorithm.

present position is replaced by the last position. It goes back to (2).

E. Torque Computation

The coenergy generated by a phase in an SRM drive is computed from

$$W'(\theta, i) = \int_0^i \psi(\theta, i) di. \tag{20}$$

The instantaneous torque produced by a phase is determined by

$$T_{\rm ph}(\theta, i) = \frac{\partial W'(\theta, i)}{\partial \theta}. \tag{21}$$

Assuming $\theta_k \le \theta \le \theta_{k+1}$ and $i_j \le i \le i_{j+1}$, and substituting (5) into (20) gives

$$\begin{aligned} W'(\theta, i) = \sum_{l=1}^{j-1} & [(c_{kl11} + c_{kl21}\theta)(i_{l+1} - i_l) \\ & + \frac{1}{2}(c_{kl12} + c_{kl22}\theta)(i_{l+1}^2 - i_l^2)] \\ & + [(c_{kj11} + c_{kj21}\theta)(i - i_j) \\ & + \frac{1}{2}(c_{kj12} + c_{kj22}\theta)(i^2 - i_j^2)]. \end{aligned} \tag{22}$$

Thus, substituting (22) into (21), we get

$$\begin{aligned} T_{\rm ph}(\theta, i) = & \sum_{l=1}^{j-1} [c_{kl21}(i_{l+1} - i_l) + \frac{1}{2} c_{kl22}(i_{l+1}^2 - i_l^2)] \\ & + [c_{kj21}(i - i_j) + \frac{1}{2} c_{kj22}(i^2 - i_j^2)]. \end{aligned} \tag{23}$$

The dynamic torque produced by an SRM drive is computed from

$$T(\theta, i) = \sum_{\rm ph=1}^{N_{\rm ph}} T_{\rm ph} \tag{24}$$

where $N_{\rm ph}$ denotes the number of phases.

It can be seen from (23) and (24) that the torque computations are the analytical expressions. Hence, the instantaneous torque in SRM drives can be computed quickly as the coefficients in (23) have been determined.

F. Salient Merits of the PSM

It can be seen from the above derivation and analysis that the developed PSM is based on the proposed hybrid model. Thus, the PSM is able to accurately describe the nonlinear magnetic characteristics in SRMs due to a larger number of fine elements when compared to those in other methods, such as analytical methods [2]–[8], interpolation methods [10]–[12] except bicubic spline interpolation, as well as equivalent magnetic circuit methods [17]–[19]. Furthermore, the conventional first-order differential voltage equation for SRM drives can be simplified into an analytical expression of the current with respect to the rotor position, which is solved using the developed PSM. The PSM does not need to solve the conventional first-order differential voltage equation when predicting the current waveforms of SRM drives, thereby eliminating the error arising from mathematically approximate algorithms used for solving first-order differential equation. Furthermore, at each step during the iteration of the PSM, it is not required to compute the current from the solved flux linkage or the inductance from the solved current. In terms of accuracy and rapidity of evaluating the solution algorithms, PSM is better than conventional algorithms, such as the Euler integration algorithm and the fourth-order Runge–Kutta algorithm, in solving the first-order differential equations.

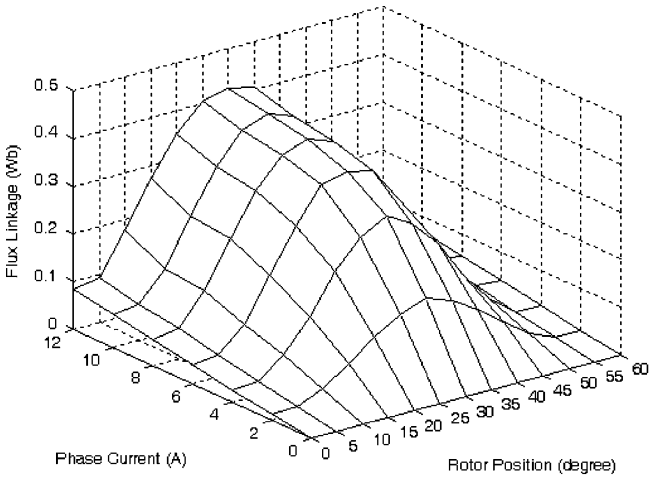

(a)

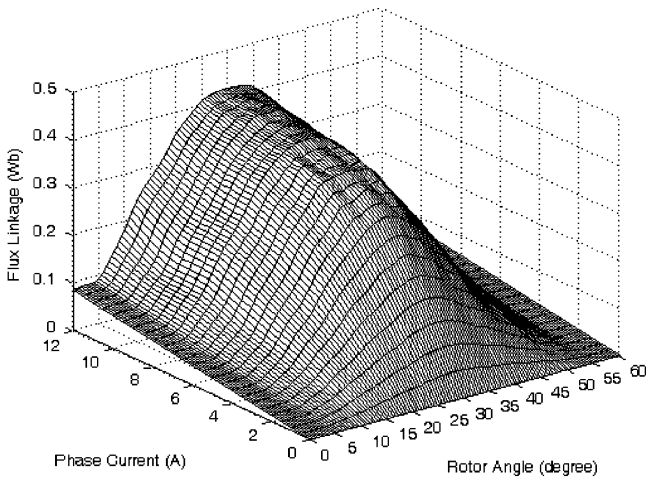

(b)

Fig. 4. Magnetic characteristics of the SRM prototype. (a) Given magnetic characteristics. (b) Rectangular elements generated by the 2-D bicubic spline interpolation.

IV. Applications

A. Simulation and Experiment

To verify the developed PSM, the operation of the prototype of a four-phase SRM drive was simulated using the developed PSM. The main data of the prototype are shown in Appendix. For the SRM prototype, the nonlinear magnetic characteristics with a small quantity of data obtained experimentally are illustrated in Fig. 4(a). Fig. 4(b) shows the distribution of the finite

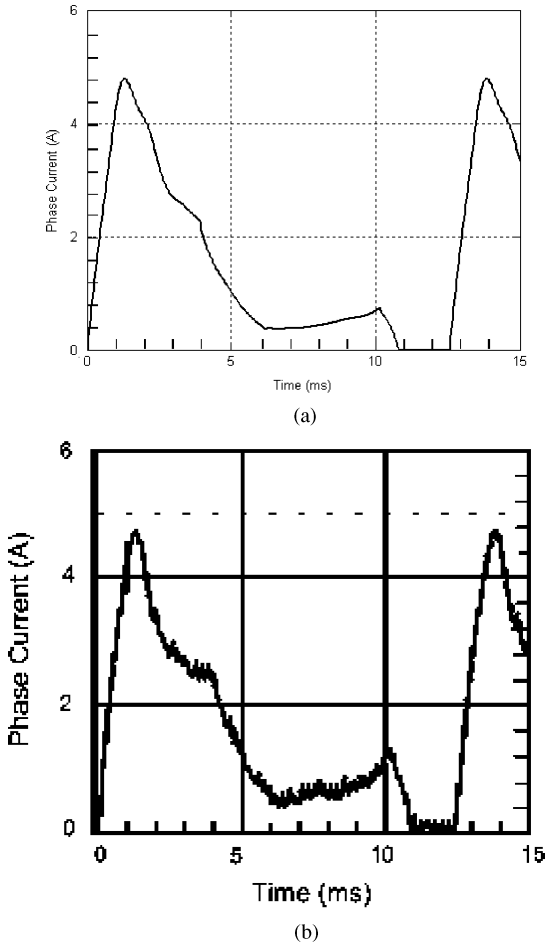

Fig. 5. Phase current waveforms under case 1. (a) Simulation by using the developed PSM. (b) Experiment.

finer elements generated by the 2-D bicubic spline interpolation, based on the given data in Fig. 4(a).

The application case 1 shows that the SRM prototype runs under the single-pulse voltage control and the operating condition is that the dc link voltage is 33.6 V, the motor speed is 800 rpm, the turn-on angle is -1°, and the conduction angle is 19°. Fig. 5 shows the current waveforms of the simulation and experiment under case 1. The application case 2 shows that the SRM prototype operates under the single-pulse voltage control, and the operating condition is that the dc link voltage is 33.6 V, the motor speed is 800 rpm, the turn-on angle is -5°, and the conduction angle is 17°. Fig. 6 depicts the current waveforms under case 2. At the same time, Figs. 7 and 8 illustrate the instantaneous torque profiles produced by the SRM using the developed torque expressions (23) and (24) and the traditional method where the numerical derivation and integration are utilized to compute (20) and (21), respectively.

B. Absolute Errors

Table I shows the distribution of the absolute errors of the current between the simulation and experimental waveforms in Fig. 5, within one period. The distribution of the absolute errors of the current between the simulation and experimental waveforms in Fig. 6 is described in Table II.

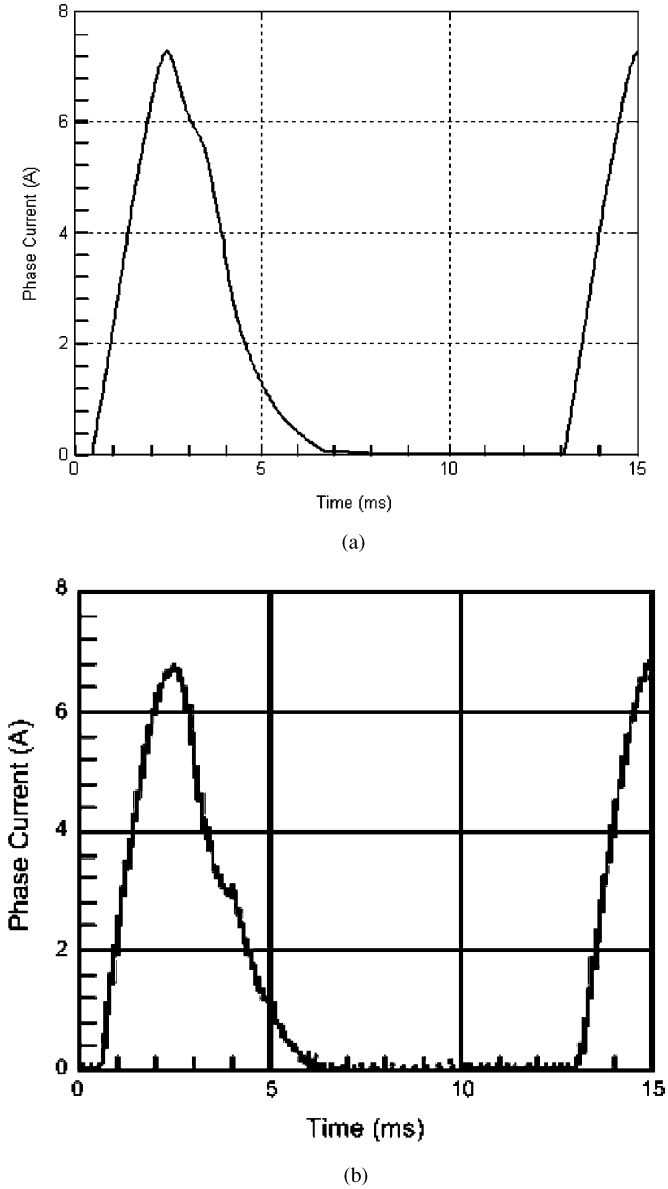

Fig. 6. Phase current waveforms under case 2. (a) Simulation by using the developed PSM. (b) Experiment.

C. PSM Validation

It can be observed from Figs. 5 and 6 that the simulated current waveforms agree fairly well with the measured current waveforms for these so-complicated waveforms. Furthermore, it can also be seen from Tables I and II that the absolute errors are small even for such complicated waveforms. On the other hand, Figs. 7 and 8 show that the instantaneous torque profiles computed by using the PSM and the traditional method are in good agreement. Hence, these findings serve as good validation for the PSM reported in this paper. They indicate that the proposed PSM is effective and correct, and that the presented hybrid model is accurate.

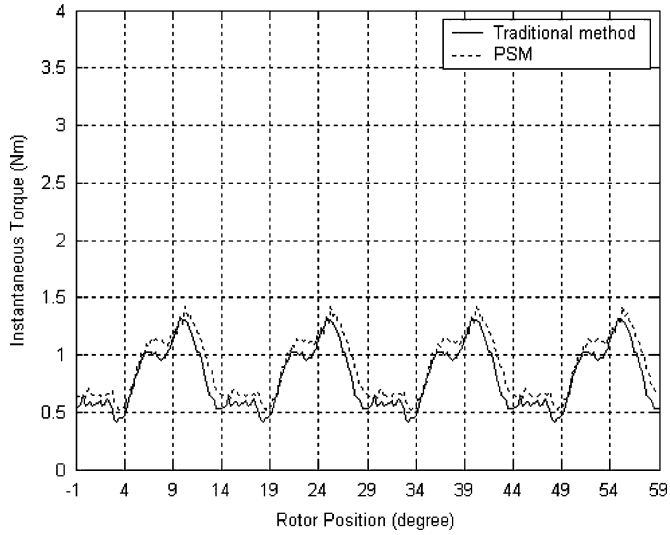

Fig. 7. Instantaneous torque profiles under case 1.

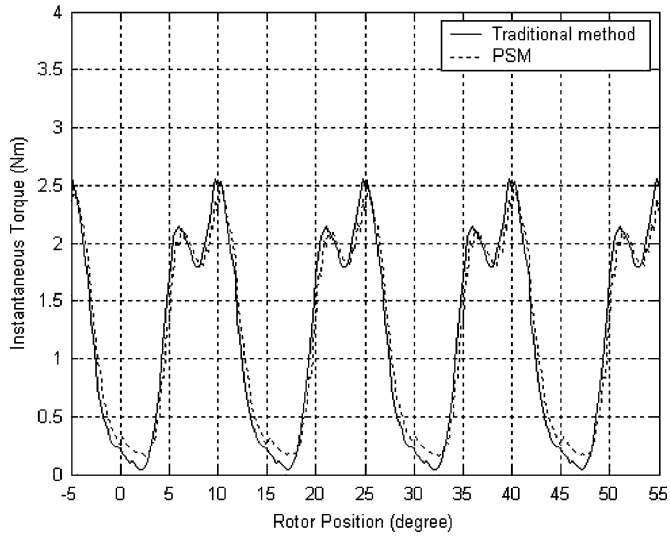

Fig. 8. Instantaneous torque profiles under case 2.

D. Computation Time

Table III shows the CPU execution time spent by the PSM and the analytical method based on the 2-D least square model [8]. Both the simulation programs are carried out on a personal computer (Intel Pentium 4/1.8 GHz CPU). It can be found from Table III that the CPU time spent by the PSM is much less than that required by the analytical method. This demonstrates that the PSM can more considerably save the simulation time when compared to other methods, such as analytical methods.

V. Conclusion

This paper has developed a novel numerical method, referred as PSM, to predict the performances of SRM drives. The PSM is based on the newly presented hybrid model of nonlinear magnetic characteristics in SRMs. A large number of fine elements generated by using the 2-D bicubic spline interpolation are able to accurately describe the nonlinear magnetic characteristics in SRMs. Due to the element shape function based on the 2-D bilinear spline function, the conventional first-order differential voltage equation is simplified into an analytical expression of the current with respect to the rotor position, which is subsequently solved using the developed position stepping algorithm.

When the currents of SRM drives are predicted, the PSM does not need to solve the conventional first-order differential voltage equation, and does not require the computation of either the current from the solved flux linkage or the inductance from the solved current at each step during the iteration. The comparisons between the simulated and measured current waveforms were reported to validate the proposed hybrid model and PSM. Furthermore, the comparisons of CPU execution time between the developed PSM and analytical method also demonstrated that the PSM requires much less time when compared to other analytical methods. Hence, the developed PSM has better accuracy and higher computation speed when compared to the traditional methods in solving the first-order differential voltage equations.

TABLE I
Absolute Errors in Fig. 5

Time (ms)	1.0	3.0	5.0	7.0	9.0
Simulation (A)	4.2659	2.6907	1.0216	0.3721	0.5383
Experiment (A)	4.20	2.60	1.10	0.45	0.65
Absolute Error (A)	0.0659	0.0907	-0.0784	-0.0779	-0.1117

TABLE II
Absolute Errors in Fig. 6

Time (ms)	1.0	2.0	3.0	4.0	5.0
Simulation (A)	2.1074	6.1244	6.2069	3.5376	1.2670
Experiment (A)	2.20	6.20	6.00	3.30	1.1
Absolute Error (A)	-0.0926	-0.0756	0.2069	0.2376	0.1670

TABLE III
CPU Execution Time of Simulation

Numerical Approach	Case-1 (s)	Case-2 (s)
Developed PSM	0.62500000E-03	0.46875000E-03
Analytical Method	0.56250000E-02	0.32812500E-02

Appendix

The main parameters of the prototype of the SRM drive are listed as follows:

1) Phases number = 4.
2) Number of stator poles = 8.
3) Number of rotor poles = 6.
4) Phase resistance = 0.687 Ω.

Phase inductance is 0.0347 H when the stator pole is aligned with the rotor pole and the phase current is equal to12 A.

Phase inductance is 0.00699 H when the stator pole is unaligned with the rotor pole and the phase current is equal to 12 A.

Phase inductance is 0.0838 H when the stator pole is aligned with the rotor pole and the phase current is equal to 2 A.

Phase inductance is 0.00632 H when the stator pole is unaligned with the rotor pole and the phase current is equal to 2 A.

REFERENCES

[1] X. D. Xue, K. W. E. Cheng, and S. L. Ho, "Correlation of modeling techniques and power factor for switched-reluctance machines drives," *Proc. Inst. Electr. Eng.-Electr. Appl.*, vol. 152, no. 3, pp. 710–722, May 2005.

[2] D. A. Torrey and J. H. Lang, "Modeling a nonlinear variable-reluctance motor drive," *Proc. Inst. Electr. Eng.*, vol. 137, no. 5, pp. 314–326, Sep. 1990.

[3] W. M. Chan and W. F. Weldon, "Development of a simple nonlinear switched reluctance motor model using measured flux linkage data and curve fit," in *Proc. 32nd IEEE IAS Annu. Meeting*, New Orleans, LA, Oct.1997, vol. 1, pp. 318–325.

[4] B. Fahimi, G. Suresh, J. Mahdavi, and M. Ehsami, "A new approach to model switched reluctance motor drive application to dynamic performance prediction, control, and design," in *Proc. 29th IEEE Annu. Power Electron. Spec. Conf.*, Fukuoka, Japan, May 1998, vol. 2, pp. 2097–2102.

[5] S. Mir, I. Husain, and M. Elbuluk, "Switched reluctance motor modeling with on-line parameter identification," *IEEE Trans. Ind. Appl.*, vol. 34, no. 4, pp. 776–783, Jul./Aug. 1998.

[6] C. Roux and M. M. Morcos, "On the use of a simplified model for switched reluctance motors," *IEEE Trans. Energy Convers.*, vol. 17, no. 3, pp. 400–405, Sep. 2002.

[7] D. N. Essah and S. D. Sudhoff, "An improved analytical model for the switched reluctance motor," *IEEE Trans. Energy Convers.*, vol. 18, no. 3, pp. 349–356, Sep. 2003.

[8] X. D. Xue, K. W. E. Cheng, and S. L. Ho, "A self-training numerical method to calculate the magnetic characteristics for switched reluctance motor drives," *IEEE Trans. Magn.*, vol. 40, no. 2, pp. 734–737, Mar. 2004.

[9] B. Loop, D. N. Essah, and S. Sudhoff, "A basis function approach to the nonlinear average value modeling of switched reluctance machines," *IEEE Trans. Energy Convers.*, vol. 21, no. 1, pp. 60–68, Mar. 2006.

[10] J. M. Stephenson and L. Corda, "Computation of torque and current in doubly-salient reluctance motors from nonlinear magnetization data," *Proc. Inst. Electr. Eng.*, vol. 126, no. 5, pp. 393–396, May 1979.

[11] D. W. J. Pulle, "New data base for switched reluctance drive simulation," *Proc. Inst. Electr. Eng.-B*, vol. 138, no. 6, pp. 331–337, Nov. 1991.

[12] S. U. Rehman and D. G. Taylor, "Piecewise modeling and optimal commutation of switched reluctance motors," in *Proc. IEEE Int. Symp. Ind. Electron.*, Athens, Greece, Jul.1995, vol. 1, pp. 266–271.

[13] X. D. Xue, K. W. E. Cheng, and S. L. Ho, "Simulation of switched reluctance motor drives using 2-D bicubic spline," *IEEE Trans. Energy Convers.*, vol. 17, no. 4, pp. 471–477, Dec. 2002.

[14] C. Elmas, S. sagiroglu, I. Colak, and G. Bal, "Modeling of a nonlinear switched reluctance drive based on artificial neural networks," in *Proc. 5th Int. Conf. Power Electron. Variable-Speed Drives*, London, U.K., Oct.1994, pp. 7–12.

[15] L. A. Belfore and A. A. Arkadan, "Modeling faulted switched reluctance motors using evolutionary neural networks," *IEEE Trans. Ind. Electron.*, vol. 44, no. 2, pp. 226–233, Apr. 1997.

[16] A. A. Arkadan, P. Du, M. Sidani, and M. Bouji, "Performance prediction of SRM drive systems under normal and fault operating conditions using GA-based Ann method," *IEEE Trans. Magn.*, vol. 36, no. 4, pp. 1945–1949, Jul. 2000.

[17] A. V. Radon, "Design considerations for the switched reluctance motor," *IEEE Trans. Ind. Appl.*, vol. 31, no. 5, pp. 1079–1087, Sep./Oct. 1995.

[18] M. Moallem and G. E. Dawson, "An improved magnetic equivalent circuit method for predicting characteristics of highly saturated electromagnetic devices," *IEEE Trans. Magn.*, vol. 34, no. 5, pp. 3632–3635, Sep. 1998.

[19] V. Vujicic and N. Vukosavic, "A simple nonlinear model of switched reluctance motor," *IEEE Trans. Energy Convers.*, vol. 15, no. 4, pp. 395–400, Dec. 2000.

[20] H. Späth, *Two Dimensional Spline Interpolation Algorithms*. Wellesley, MA: Peters, 1995.

X. D. Xue received the Bachelor's degree from Hefei University of Technology, Hefei, China, in 1984, the Master's degree from Tianjin University, Tianjin, China, in 1987, and the Ph.D. degree from the Hong Kong Polytechnic University, kowloon, Hong Kong, in 2004, all in electrical engineering.

From 1987 to 2001, he was engaged in teaching and research in the Department of Electrical Engineering, Tianjin University. He is currently with the Department of Electrical Engineering, Hong Kong Polytechnic University. His current research interests include electrical machines, electrical drives, and power electronics.

K. W. E. Cheng (M'90–SM'06) received the B.Sc. and Ph.D. degrees in electrical engineering from the University of Bath, Bath, U.K., in 1987 and 1990, respectively.

He was a Principal Engineer with Lucas Aerospace, Birmingham, U.K., where he led a number of power electronics projects. In 1997, he joined the Hong Kong Polytechnic University, Kowloon, Hong Kong, where he is currently a Professor and the Director of the Power Electronics Research Centre. His current research interests include all aspects of power electronics. He is the author or coauthor of more than 200 published papers and seven books.

Prof. Cheng received the Institution of Electrical Engineering (IEE) Sebastian Z De Ferranti Premium Award in 1995, the Outstanding Consultancy Award in 2000, the Faculty Merit Award for Best Teaching in 2003, and the Research and Scholarly Activities Award from the Hong Kong Polytechnic University in 2006.

S. L. Ho received the B.Sc. and Ph.D. degrees in electrical engineering from the University of Warwick, Coventry, U.K., in 1976 and 1979, respectively.

In 1979, he joined the Hong Kong Polytechnic University, Kowloon, Hong Kong, where he is currently the Chair Professor of electrical utilization and the Head of the Department of Electrical Engineering. He has been engaged in the local industry, particularly in railway engineering. He is the holder of several patents, and is the author or coauthor of more than 100 papers published in leading journals, mostly in the IEEE TRANSACTIONS and the *Institution of Electrical Engineering Proceedings*. His current research interests include traction engineering, application of finite elements in electrical machines, phantom loading of machines, and optimization of electromagnetic devices.

Prof. Ho is a member of the Institution of Electrical Engineers, U.K., and the Hong Kong Institution of Engineers.